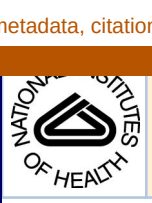

Published in final edited form as:
Mol Cell Neurosci. 2014 September ; 62: 10–18. doi:10.1016/j.mcn.2014.07.004.

Regulation of Voltage-Gated Ca^{2+} Currents by Ca^{2+}/Calmodulin-dependent Protein Kinase II in Resting Sensory Neurons

Sandra Kostic, PhD[1],
Research Fellow, Medical College of Wisconsin, Department of Anesthesiology, 8701 Watertown Plank Road, Milwaukee, WI 53226, USA

Bin Pan, PhD,
Research Scientist, Medical College of Wisconsin, Department of Anesthesiology, 8701 Watertown Plank Road, Milwaukee, WI 53226, USA

Yuan Guo, PhD,
Research Fellow, Medical College of Wisconsin, Department of Anesthesiology, 8701 Watertown Plank Road, Milwaukee, WI 53226, USA

Hongwei Yu, MD, MS,
Assistant Professor, Medical College of Wisconsin, Department of Anesthesiology, 8701 Watertown Plank Road, Milwaukee, WI 53226, USA

Damir Sapunar, MD, PhD,
Department of Anatomy, Histology and Embryology, University of Split School of Medicine, Split, Croatia

Wai-Meng Kwok, PhD,
Professor, Medical College of Wisconsin, Department of Anesthesiology, 8701 Watertown Plank Road, Milwaukee, WI 53226, USA

Andy Hudmon, PhD,
Associate Professor, Indiana University School of Medicine, Department of Biochemistry and Molecular Biology-Stark Neuroscience Research Institute, 950 West Walnut (R2-480), Indianapolis, IN 46202, USA

Hsiang-En Wu, MD, and
Assistant Professor, Medical College of Wisconsin, Department of Anesthesiology, 8701 Watertown Plank Road, Milwaukee, WI 53226, USA

Quinn H. Hogan, MD
Professor, Medical College of Wisconsin, Department of Anesthesiology, 8701 Watertown Plank Road, Milwaukee, WI 53226, USA; Anesthesiologist, Zablocki VA Medical Center, 5000 W. National Avenue, Milwaukee, WI 53295, USA

Corresponding Author: Quinn H. Hogan, MD, phone (414) 456-5727.
[1]Present address: Department of Anatomy, Histology and Embryology, University of Split School of Medicine, Split, Croatia.

Sandra Kostic: sandra.kostic@mefst.hr; Bin Pan: bpan@mcw.edu; Yuan Guo: guoy@mcw.edu; Hongwei Yu: hyu@mcw.edu; Damir Sapunar: damir.sapunar@mefst.hr; Wai-Meng Kwok: wmkwok@mcw.edu; Andy Hudmon: ahudmon@iu.edu; Hsiang-En Wu: hwu@mcw.edu; Quinn H. Hogan: qhogan@mcw.edu

Abstract

Calcium/calmodulin-dependent protein kinase II (CaMKII) is recognized as a key element in encoding depolarization activity of excitable cells into facilitated voltage-gated Ca^{2+} channel (VGCC) function. Less is known about the participation of CaMKII in regulating VGCCs in resting cells. We examined constitutive CaMKII control of Ca^{2+} currents in peripheral sensory neurons acutely isolated from dorsal root ganglia (DRGs) of adult rats. The small molecule CaMKII inhibitor KN-93 (1.0μM) reduced depolarization-induced I_{Ca} by 16 – 30% in excess of the effects produced by the inactive homolog KN-92. The specificity of CaMKII inhibition on VGCC function was shown by efficacy of the selective CaMKII blocking peptide autocamtide-2-related inhibitory peptide in a membrane-permeable myristoylated form, which also reduced VGCC current in resting neurons. Loss of VGCC currents is primarily due to reduced N-type current, as application of mAIP selectively reduced N-type current by approximately 30%, and prior N-type current inhibition eliminated the effect of mAIP on VGCCs, while prior block of L-type channels did not reduce the effect of mAIP on total I_{Ca}. T-type currents were not affected by mAIP in resting DRG neurons. Transduction of sensory neurons *in vivo* by DRG injection of an adeno-associated virus expressing AIP also resulted in a loss of N-type currents. Together, these findings reveal a novel molecular adaptation whereby sensory neurons retain CaMKII support of VGCCs despite remaining quiescent.

Keywords

Calcium/calmodulin-dependent protein kinase II; sensory neuron; voltage-gated calcium channel; calcium signaling

INTRODUCTION

Voltage-gated Ca^{2+} channels (VGCCs) are the dominant path of activity-related Ca^{2+} entry in most neurons, and thereby drive critical functions including synaptic transmission and regulation of neuronal excitability (Berridge, 1998). Sensory neurons are equipped with a broad range of VGCCs, including high-voltage-activated (HVA) channels as well as those that open at low voltages (LVA). Recordings from sensory neurons, typically in somata dissociated from the dorsal root ganglia (DRGs), demonstrate multiple subtypes of HVA channels (McCallum et al., 2011). The largest currents are conducted through the conotoxin-sensitive N-type channels that incorporate the pore-forming α_1 subunit designated $Ca_V2.2$, and dihydropyridine-sensitive L-type channels ($Ca_V1.2$ and 1.3). Smaller components of the overall ensemble of voltage-gated I_{Ca} are contributed by P/Q-type ($Ca_V2.1$) that is sensitive to agatoxin, R-type HVA current ($Ca_V2.3$) that is sensitive to toxin from tarantula venom, and T-type LVA current ($Ca_V3.2$). Some distinct roles have been defined for particular VGCC subtypes. Specifically, N-type current is the dominant source of Ca^{2+} influx for dorsal horn neurotransmission in pain pathways (Heinke et al., 2004), while P/Q-type current mediates synaptic transmission between inhibitory interneurons and dorsal horn neurons (Takahashi and Momiyama, 1993). L-type current is particularly linked to signaling

that triggers gene expression (Fossat et al., 2010), and T-type current supports repetitive firing (Nelson et al., 2005).

Modulation of VGCC function underlies both physiological regulation of channel operation as well as pathogenic alterations (Park and Luo, 2010). Sensitivity to G-protein (Park and Luo, 2010) and kinase signaling systems, including Ca^{2+}-sensitive kinases that provide feedback regulation, are well established as pathways modulating VGCCs. A central role for the serine/threonine protein kinase, Ca^{2+}/calmodulin-dependent protein kinase II (CaMKII) in Ca^{2+} regulation of VGCCs is suggested by its abundance in neurons, as well as identification of CaMKII phosphorylation sites on the pore-forming α1 subunits of N- and L-type channels (Hell et al., 1994; Hell et al., 1993). Furthermore, CaMKII enhances L- and P/Q-type currents through both phosphorylation and structural interactions (Blaich et al., 2010; Dzhura et al., 2000; Grueter et al., 2006; Hudmon et al., 2005; Jiang et al., 2008; Lee et al., 2006). We have recently observed that sensory neuron activation results in CaMKII-dependent facilitation of N-type I_{Ca}, which in turn results in a period of depressed neuronal excitability (Tang et al., 2012). Since the regulation by CaMKII of neuronal VGCCs in the resting state has only been minimally examined (P/Q currents in hippocampal neurons (Jiang et al., 2008)), the experiments reported here were designed to identify if CaMKII provides constitutive control over VGCC function in sensory neurons in the absence of prior neuronal firing.

METHODS

Recombinant adeno-associated virus (AAV) vectors

An AAV vector was designed to encode a chimeric protein in which enhanced GFP (EGFP) was linked to the CaMKII inhibiting peptide autocamtide-2-related inhibitory peptide (AIP) (Ishida and Fujisawa, 1995). A DNA fragment containing the EGFP-AIP sequence from pEGFPc1-AIP (kindly provided by Dr. Steven H. Green, Department of Biological Sciences, University of Iowa (Bok et al., 2007)) was cloned into the *Nde*I/*Hpa*I sites of pAAV-DS-CMV, a double-strand serotype 8 AAV plasmid (Viromics, Fremont, CA), to generate pdsAAV-CMV-EGFP-AIP. EGFP released from pEGFP-c1 was cloned into pAAV-DS-CMV to generate pdsAAV-CMV-EGFP. AAV vectors of AAV8-EGFP-AIP and AAV8-EGFP were produced in our laboratory by the triple-transfection of either pdsAAV-CMV-EGFP-AIP or pdsAAV-CMV-GFP (control) with pRC8 and pHelpler (Viromics) into 293T cells, followed by two cycles of cesium chloride gradient purification and concentrated as previously described (Grimm et al., 2003). Encapsidated DNA was quantified by a PicoGreen assay (Invitrogen, Carlsbad, CA) following denaturation of the AAV particles, and the physical titer was calculated and expressed as genome copy number per ml (GC/ml). The titers of AAV8-EGFP-AIP and AAV8-EGFP were 3.04×10^{12} GC/ml and 9.84×10^{12} GC/ml, respectively.

Animal preparation

All animal experiments were approved by the Medical College of Wisconsin Animal Care and Use Committee. A total of 70 male Sprague-Dawley rats (Taconic, Hudson, NY, USA) weighing 125–150 g were used. Rats were housed in individual cages under controlled

conditions, with food and water available *ad libitum*. Control animals received midline lumbar skin incision during brief general anesthesia (Isoflurane 2% in O_2). Other rats were injected with vectors AAV8-EGFP or AAV8-EGFP-AIP, as described previously (Fischer et al., 2011). Briefly, after exposure through a midline lumbar incision, the intervertebral foramen was enlarged by removal of laminar bone to expose the distal pole of the right 4th lumbar (L4) and L5 DRGs. A pulled glass micropipette was advanced through the capsule into the ganglion. Injection of vectors (2×10^9 viral particle in 2μl per DRG) was performed over a 5min period using a microprocessor-controlled injector (World Precision Instruments, Sarasota, FL, USA). This volume has been demonstrated to fill the DRG without spilling into adjacent tissues (Fischer et al., 2011).

Neuronal dissociation

The L4 and L5 DRGs were harvested and dissociated 3 weeks after surgery in control and injected rats. After decapitation under deep isoflurane anesthesia, DRGs were removed and placed into a 35 mm Petri dish containing Ca_2/Mg_2-free, iced Hank's balanced salt solution – HBSS (Gibco, Life Technologies Corp, Brown Deer WI). The ganglia were cut into several pieces, incubated for 25 min at 37°C in 0.5 mg/ml Liberase TM (Roche) in DMEM/F12 (1:1) DMEM/Ham's F12 (Gibco), resuspended for 10 min at 37°C in 1 mg/ml trypsin (Sigma–Aldrich, St. Louis MO) and 15K Kunitz units DNase (Sigma–Aldrich). Dissociated neurons were then placed in 0.1% trypsin inhibitor (Type II, Sigma–Aldrich), centrifuged and lightly triturated in neural basal media (Gibco) containing 2% (v:v) B27 supplement (Gibco), 0.5 mM L-glutamine (G-7029, Sigma–Aldrich), 0.05 mg/ml gentamicin (Gibco), 10 ng/ml nerve growth factor 7S (Alomone Labs Ltd., Jerusalem, Israel), and 1.8mM Ca^{2+} concentration. Cells were then plated onto glass coverslips (Carolina Biological Supply, Burlington, NC) coated with poly-L-lysine (70–150 kDa, Sigma–Aldrich), and cultured at 37°C in humidified 95% air and 5% CO_2 for at least 2 h. Cells were used within 3–8 h after dissociation.

Whole cell patch clamp recording

Currents were recorded in the whole-cell configuration of the patch-clamp technique. Patch pipettes, ranging from 2 to 4 MΩ resistance, were formed from borosilicate glass (King Precision Glass, Inc, Claremont, CA) and fire polished. Currents were recorded with an Axopatch 200B amplifier (Molecular Devices, Sunnyvale, CA), filtered at 2 kHz through a 4-pole Bessel filter, and digitized at 10 kHz with a Digidata 1320 A/D interface and pClamp 9 software (Molecular Devices). Gigaohm seals were achieved in modified Tyrode's solution containing (in mM): 140 NaCl, 4 KCl, 2 $CaCl_2$, 2 $MgCl_2$, 10 D-glucose, and 10 HEPES, pH of 7.4, with an osmolarity of 300 mOsm. Access resistance was 80–90% compensated. Voltage-induced currents flowing through Ca^{2+} channels were then isolated and recorded using an extracellular solution containing (in mM): 2 $BaCl_2$, 5 4-aminophyridine, 10 HEPES, 132 N-methyl-D-glucamine, 4.8 CsCl, 5 Glucose, 2 $MgCl_2$, pH of 7.4, with an osmolarity of 300 mOsm. Although Ba^{2+} was the charge carrier, we hereafter refer to currents as I_{Ca}. The internal pipette solution contained (in mM): 110 CsCl, 20 TEACl, 5 Mg-ATP, 0.4 Li_4-GTP, 11 EGTA (unless otherwise noted), 1 $CaCl_2$, 1 $MgCl_2$, 0.1 c-AMP, and 10 HEPES, pH of 7.2, with an osmolarity of 300 mOsm. To selectively record low-voltage-activated T-type currents, we used a pipette solution that contained fluoride to

facilitate high-voltage-activated I_{Ca} rundown (Todorovic and Lingle, 1998). This solution contained tetramethylammonium hydroxide (TMA-OH) 135, EGTA 10, HEPES 40, and $MgCl_2$ 2, adjusted to pH 7.2 with hydrofluoric acid, and with an osmolarity of 300mOsm.

Currents were activated by voltage commands in consisting of either step depolarizations or action potential (AP) waveform depolarizations. After a test depolarization at least 1min of membrane rest elapsed before a subsequent test depolarization. Data from whole-cell I_{Ca} recordings were evaluated with Axograph X 1.3.5 (AxoGraph Scientific, Sydney, Australia), with which peak inward currents were measured. The density of currents was determined by normalizing peak current to cell capacitance (pA/pF). Current-voltage (I-V) data from recordings during step depolarizations were fit to a Boltzmann equation in the form:

$$I_{Ba} = \frac{G_{Max}(V_M - V_R)}{1+\exp(V_M - V_{\frac{1}{2}}/k)}$$

where I_{Ba} is current (not leak subtracted), G_{Max} is the maximum channel conductance, $V_{1/2}$ is the voltage at which current is half maximal, k is a slope factor describing voltage dependence of conductance, V_R is the reversal potential for current, and V_M is the membrane potential, determined separately for each cell, using Prism v. 4 (GraphPad Software, Inc., San Diego, CA).

CaMKII catalytic assay

Following cardiac perfusion with a solution designed to avoid activation of CaMKII in sensory neurons (in mM: 26 $NaHCO_3$, 1.9 KCl, 1.3 $MgSO_4$, 1.2 KH_2PO_4, 10 glucose, 1 EGTA, 254 sucrose aerated with 5% CO_2 in oxygen, at 25°C), the L4 and L5 DRGs were removed bilaterally from a control rat three days after skin incision and were homogenized in 150μl of lysis buffer (Kolb et al., 1995) containing 2X protease inhibitors (Millipore, 539137) and 2X phosphatase inhibitors (Millipore, 524624), and incubated on ice for 30 minutes. The pooled lysate was spun down at 14000 rpm for 10 min at 4°C. To determine the level of CaMKII catalytic activity, the sample was analyzed for the ability to phosphorylate the specific CaMKII substrate AC-2 (KKALRRQETVDAL) in the presence of 1mM Ca^{2+} and 5 μM calmodulin and [γ-^{32}P]ATP (3 μCi per reaction) or 10 mM EGTA as described previously (Kolb et al., 1995) for autonomous activity determination. The reaction mixtures were spotted onto P81 phosphocellulose paper and the excess free-labeled ATP γP^{32} was washed off by rinsing the spotted sheet (Ashpole and Hudmon 2011). Phosphorylated AC-2 (P^{32} labeled) was measured using Cerenkov counting in a scintillation counter. The background readings for each lysate (complete reactions minus AC-2) were subtracted for the Ca^{2+}-induced kinase activity and autonomous activity determinations. The autonomous activity is calculated as the percentage of activity in the presence of EGTA divided by total activity induced with saturating levels of Ca^{2+}/calmodulin in the lysate.

Agents

All chemicals were obtained from Sigma Aldrich unless otherwise specified. Two conventional and distinct CaMKII inhibitors were employed. KN-93 was compared to its inactive isomer KN-92 (Calbiochem, EMD Millipore Corporation, Billerica, MA), while the

selective peptide inhibitor AIP was used in its membrane-permeable myristoylated form (mAIP, Calbiochem), with myristoyl-chloride (mCl) as a control, both at 5μM. HVA Ca^{2+} channel subtypes were isolated using selective blockers. Nisoldipine (Peptides International, Louisville, KY) or nimodipine (Calbiochem) were used to block L-type current, SNX- 111 (synthetic ω-conotoxin MVIIA, Peptides International, Louisville, KY) to block N-type current, ω-conotoxin MVIIC (MVIIC) for irreversible blockade of P/Q type currents and reversible block of N-type. SNX-482 (Peptides International) blocks residual R-type current. Non-saturating doses of these blockers were used to avoid non-specific effects (McCallum et al., 2011), and about 20% of HVA I_{Ca} in DRG neurons remained unaffected after their combined application, which was sensitive to the non-selective I_{Ca} blocker cadmium (200 μM, data not shown). Antagonists were delivered in the external Ba^{2+} solution directly to the neuron through a pressure regulated microperfusion system (ALA-BP8 system, ALA Scientific, Farmingdale, NY). Each neuron was exposed to only one concentration of blocker.

KN-93 stock solution was dissolved in water, aliquoted and kept at −20°C until use. KN-92 was dissolved in DMSO and aliquoted and kept at −20°C. DMSO was present in final solutions at a concentration 0.1%. This concentration had no effect on I_{Ca} when administered alone (rundown with DMSO of 20.9±1.4% after 8min, n=5; without DMSO 20.3±2.8%, n=8; P=0.89), or when included in trials of KN-93 (n=5, with EGTA at 11mM), so these data were pooled with data from DMSO-free Control or KN-93 data, respectively. mAIP and mCl were dissolved in water, aliquoted and stored on −20°C. Nisoldipine was dissolved in DMSO and stored at +4°C. SNX-111, SNX-482 and MVIIC were diluted in water, lyophilized, and aliquots were stored at −80°C.

Analysis and statistics

To test statistical significance of differences between groups, one-way or two-way ANOVA was performed where appropriate and *post hoc* paired comparisons were performed with Tukey's test using Prism (GraphPad Software). Where appropriate, 2-tailed t-tests were used to compare findings before and after applications of agents or between groups, calculated with Excel (Microsoft, Redmond WA). Data are presented as mean ± SEM. Effects are considered significant for $P<0.05$.

RESULTS

Neuronal Activity

Dissociated sensory neurons are inactive unless depolarized from their natural resting membrane potential, accurately reflecting the behavior of healthy sensory neurons *in situ* (Bessou and Perl, 1969). In the present study, no spontaneous firing was observed throughout the recording period of all neurons.

Effect on I_{Ca} of CaMKII inhibition by brief KN-93 application

In order to explore the effect of CaMKII regulation of I_{Ca} in resting peripheral sensory neurons, we first employed the conventional CaMKII inhibitor KN-93 (1 μM, Fig. 1A), which as an allosteric inhibitor prevents Ca^{2+}-dependent CaMKII activation and

autophosphorylation. In parallel, other neurons were exposed to the inactive isomer KN-92 to identify off-target effects of KN-93. Current rundown was monitored in neurons not receiving either agent (Fig. 1B). Time of exposure for recording the response of I_{Ca} to these conditions was chosen as 5min to balance allow development of the differential effect of KN-93 *vs.* KN-92 while limiting progressive development of current rundown (Fig. 1B). To maintain resting $[Ca^{2+}]_c$ conditions throughout the recording, we buffered the internal (pipette) solution with 2.2mM EGTA, which produced a calculated free Ca^{2+} concentration of 149nM (http://maxchelator.stanford.edu) that is typical of resting sensory neurons (Fuchs et al., 2005). Under these conditions, the inactive compound KN-92 did not influence I_{Ca}, whereas the active CaMKII inhibitor KN-93 depressed I_{Ca} in excess of the influence of I_{Ca} rundown (Fig. 1B, C).

Neuronal activation in a Ba^{2+} bath solution may lead to cyotplasmic accumulation of Ba^{2+} without subsequent clearance (Mironov and Usachev, 1990), which may affect cellular processes such as secretion (TerBush and Holz, 1992), Ca^{2+} release from stores (Hardcastle et al., 1985), and VGCC function (Tang et al., 2012). To limit Ba^{2+} accumulation and to assure that any Ca^{2+} released from stores did not participate in CaMKII activation, we also tested the effect of KN-93 during greater divalent cation buffering (TerBush and Holz, 1992). With a pipette solution containing 11mM EGTA, calculated free Ca^{2+} was 21nM, and a total Ba^{2+} load as large as 1μM would result in a free Ba^{2+} level of only 7.4nM. Under these conditions, we confirmed that KN-93 (1μM) reduced I_{Ca} while KN-92 had no effect (Fig. 1D). Additional buffering (pipette Ca^{2+} to 6nM) using BAPTA produced comparable results (Fig. 1E). These data indicate that I_{Ca} is sensitive to KN-93 inhibition of CaMKII across a range of experimental conditions, and indicate that ongoing Ca^{2+}-CaM-dependent activation of CaMKII is necessary to maintain VGCC function in sensory neurons at rest.

Effect on I_{Ca} of CaMKII inhibition by mAIP application

In addition to the small molecule inhibitor KN-93, we also tested if a cell permeable peptide CaMKII inhibitor led to alterations in I_{Ca}. A myristoylated form of the CaMKII inhibitor AIP (Ishida et al., 1995) mimicking the autoinhibitory domain of CaMKII was selected because it inhibits both CaMKII activation and autophosphorylated CaMKII. Bath application of mAIP (5 μM) produced a time-dependent reduction of I_{Ca} in excess of that seen in time controls or in neurons exposed to mCl (Fig. $2A_1$). After 2min of application, at which time the selective effect of mAIP was maximal, it produced an approximately 21% reduction in peak I_{Ca} induced by step depolarizations, whereas less than 5% I_{Ca} rundown was seen with both mCl and vehicle (Fig. $2A_2$). The specific action of both KN-93 and mAIP versus their control agents indicates that that CaMKII regulates voltage-gated I_{Ca} in resting sensory neurons.

Since neuronal activation during DRG harvest could be a source of CaMKII activation and thereby may artifactually disrupt baseline CaMKII signaling, we harvested additional DRGs after initiating cardiac perfusion with ice-cold artificial CSF solution containing (in mM): 2.5 KCl, 0.5 $CaCl_2$, 7 $MgSO_4$, 1.25 NaH_2PO_4, 26 $NaHCO_3$, 2 EGTA, 25 Glucose, and 230 sucrose, saturated with 95% O_2 and 5% CO_2. The response to mAIP in these neurons did (Fig. $2A_2$) not differ from recordings made in neurons harvested in the conventional way.

We additionally tested CaMKII blockade under more physiological conditions using Ca^{2+} as the charge carrier in the bath (Fig. $2A_3$), and identified a persisting, although reduced, effect of mAIP on I_{Ca} under these conditions.

The normal action potential (AP) of sensory neuron somata is only a few milliseconds long (Sapunar et al., 2005), so conventional step depolarizations lasting hundreds of milliseconds do not reflect the typical depolarization encountered by a resting neuron. Accordingly, the effects of mAIP and mCl were additionally tested using an AP waveform voltage command, delivered to resting neurons. The temporal pattern of I_{Ca} evoked in this fashion matched prior observations, with peak inward current occurring during the repolarizing limb of the AP (Fig. $2B_1$). Two measurements were made to characterize I_{Ca} elicited by an AP-waveform command. Peak I_{Ca} amplitude was inhibited by mAIP, but not by mCl (Fig. $2B_2$). Similarly, the total charge transfer Q_{Ca}, determined as the area under the curve for I_{Ca} against time, was inhibited only by mAIP (Fig. $2B_3$). These findings indicate that CaMKII regulates currents generated when a resting sensory neuron is activated in a physiologically relevant fashion.

In addition to the effects we had so far observed with CaMKII inhibition for 2 to 5 minutes, we also considered whether there might be a mode of action of CaMKII that takes longer to reverse. We therefore examined total I_{Ca} induced by step depolarization in resting neurons that had been incubated in mAIP (5μM) for 2 hours, and compared to neurons incubated in the same concentration of mCl, as well as time controls. Under these conditions, peak current was depressed by mAIP, whereas mCl had no effect (Fig. 2C). The approximate 29% depression of I_{Ca} by mAIP in this incubation experiment is somewhat larger than the approximately 21% loss of current in the 2 minute application, suggesting that prolonged CaMKII suppression may further reduce I_{Ca}, although direct statistical comparison between these protocols is not possible.

Effect of CaMKII inhibition on biophysical parameters of I_{Ca}

As a first step in characterizing the mechanism of CaMKII action on VGCCs, we examined the influence of CaMKII inhibition on voltage and conductance parameters derived from Boltzmann analysis. Boltzmann fit of the averaged normalized currents (Fig. 3A) showed a small depolarizing shift in $V_{1/2}$ for I_{Ca} activation after mAIP application compared to mCl application and time controls, with no effect on slope factor k. Further analysis of the influence of mAIP by determining Boltzmann parameters for each neuron showed that mAIP reduced G_{Max} by 0.37±0.10pS/pF (n=12), in contrast to time controls (reduced by 0.08±0.05pS/pF, n=16; $P<0.01$ *vs.* mAIP), whereas there was no difference from controls in neurons treated with mCl (reduced by 0.20±0.04pS/pF, n=14). This analysis confirms the reduction in peak currents noted above. There was no effect of CaMKII inhibition on V_R or k (data not shown). A small depolarizing shift of $V_{1/2}$ for channel activation was confirmed during mAIP application (1.9±0.6mV, n=12), in contrast to controls (decreased 1.4±0.4mV, n=16; $P<0.001$) and mCl (decreased 2.3±0.3mV, n=14; $P<0.001$). The small extent of this shift suggests that the predominant effect of CaMKII upon VGCCs involves modulation of channel conductance or open probability.

Subtypes of I_{Ca} sensitive to CaMKII action

We next sought to distinguish the effects of CaMKII inhibition upon distinct VGCC subtypes to identify if CaMKII action is necessary for maintaining performance of all, or only a subset, of specific VGCCs in resting sensory neurons. Low-voltage-activated (LVA) T-type currents are present in sensory neurons, in which they support excitability (McCallum et al., 2003; Nelson et al., 2005). We therefore examined the effect of mAIP upon T-type I_{Ca}, isolated by application HVA current blockers and evoked by depolarizations to −30mV. Despite previous findings for CaMKII regulation of LVA currents in expression systems (Welsby et al., 2003; Wolfe et al., 2002), we did not observe that CaMKII activity was required for full expression of resting LVA currents in sensory neurons (Fig. 3B).

Our previous investigations showed that CaMKII-dependent facilitation of I_{Ca} following intense neuronal activity depended specifically upon N-type channels (Tang et al., 2012). To identify whether the actions of CaMKII in resting sensory neurons are VGCC subtype specific, we examined the sensitivity to mAIP of N-type and L-type currents, which constitute the majority of sensory neuron I_{Ca} (McCallum et al., 2011). To isolate N-type current, neurons were incubated (30min) in a combination of agents that blocked other subtypes (nisoldipine for L-type, SNX-482 for R-type, and temporary application of ω-conotoxin MVIIC for P/Q type). Thereafter, application of mAIP eliminated 24.2±2.6% of the residual current evoked by step depolarizations, whereas time controls showed only a 3.1±2.8% current loss ($P<0.001$). Because mCl produced no effects in any prior experiments, mCl was not further examined as a control. Subsequent application of N-type blocker SNX-111 (200nM, 5min) eliminated all but 18.7±2.6% of the pre-mAIP baseline current and 24.1±2.3% in time controls (n.s.). We calculated the action of mAIP selectively on N-type current by excluding the I_{Ca} that remained following terminal SNX-111 application, which showed significant suppression by mAIP for step depolarizations, as well as for N-type current evoked by AP-waveform commands (Fig. 3C).

As a complementary approach, we next eliminated N-type current by SNX-111 application and then examined the sensitivity of the remaining current to mAIP. SNX-111 blocked a major component of total I_{Ca} (during step depolarization, 63.4±1.8% of peak current, n=15; during AP-waveform depolarization, 67.9±1.6% of peak current and 67.5±1.6% of Q_{Ca}, n=15). Application of mAIP thereafter had no effect (Fig. 3D), indicating that N-type block precludes the effect of CaMKII inhibition. We also performed the reciprocal experiment of first blocking L-type current. Nisoldipine blocked 26.7±2.3% of I_{Ca} induced by step depolarizations (n=32), after which mAIP still reduced the residual current by approximately 25% of (Fig. 3E). In a small number of neurons depolarized by AP waveforms, depression of I_{Ca} by mAIP (19.0±0.7% of peak current and 31.5±0.6% of Q_{Ca}, n=3) was similarly retained following nisoldipine treatment. Together, these findings indicate that the dominant effect of CaMKII is on N-type currents.

Previous work on hippocampal pyramidal neurons has shown that CaMKII has an important effect on channel kinetics such that inhibiting CaMKII accelerates P/Q-type I_{Ca} inactivation of $Ca_V2.1$ (P/Q-type) current during step depolarization of a resting neuron (Jiang et al., 2008). To identify if the same is true regarding the action of CaMKII on N-type current in

resting sensory neurons, we evaluated the fraction of peak current remaining after 500ms depolarization in isolated N-type current, both before and after application of mAIP. No change was seen in the fraction of sustained current for either mAIP (0.71±0.02 before mAIP, 0.68±0.02 after mAIP, n=10, P=0.24) or in time controls (0.72±0.01 first determination, 0.72±0.02 second determination, n=12; P=0.96). This indicates that CaMKII had no evident effect on N-type channel kinetics in resting neurons, and that the CaMKII modulates activity-induced Ca^{2+} influx predominantly through its regulation of conductance through N-type channels.

Effect on I_{Ca} of *in vivo* CaMKII inhibition by EGFP-AIP expression

To expand upon our findings from the pharmacological approaches on dissociated sensory neurons reported above, we employed a model (Fig. 4A) in which neuronal expression of AIP is induced *in vivo* through DRG injection of AAV vector in adult rats, thereby exposing VGCCs *in situ* to AIP expression for 3 weeks prior to dissociation for electrophysiological recording. This EGFP-AIP construct has previously been shown to suppress activity-induced CaMKII action in sensory neurons (Tang et al., 2012). Control animals were subjected to neuronal transduction in an identical fashion except that the transgene product consisted of EGFP without the AIP peptide. A scrambled peptide was not used because of prior validation of this construct (Bok et al., 2007; Tang et al., 2012) and the uncertain inactivity of scrambled peptides. To confirm successful inhibition of CaMKII activity by the EGFP-AIP transgene product, we compared the sensitivity of I_{Ca} to CaMKII blockade (bath-applied mAIP) in neurons transduced by either EGFP-AIP *versus* EGFP vectors. This showed only minimal residual CaMKII activity in neurons expressing EGFP-AIP (Fig. 4B).

Using this system, baseline I_{Ca} measures were not affected by transgene expression (Fig. 4C, D). On the basis of the particular dependence of N-type current on CaMKII identified above and in prior experiments (Tang et al., 2012), we measured the portion of I_{Ca} in these neurons that was sensitive to SNX-111. This revealed a 20% depression of N-type I_{Ca} in neurons expressing EGFP-AIP compared to EGFP alone, by all three measures (Fig. 4E). Boltzmann analysis of this SNX-111-sensitive (N-type) component showed no effect of CaMKII inhibition by AIP on $V_{1/2}$ or k (data not shown), confirming findings reported above from acute application mAIP. Additionally, the extent of N-type (SNX-111 sensitive) I_{Ca} inactivation during the 500ms step depolarization did not differ between the two vectors (for EGFP-AIP, 0.48±0.05 fraction of sustained current, n=8; for EGFP, 0.53±0.05, n=13; P=0.46), confirming our observation during acute mAIP application (above) that CaMKII does not regulate N-type inactivation kinetics in resting neurons. Overall, these findings indicate that sustained *in vivo* inhibition of CaMKII diminishes N-type I_{Ca} in resting sensory neurons, which is accompanied by compensatory increase of other VGCC subtypes.

CaMKII activity in resting sensory neurons

Our findings imply that there is active (phosphorylated) CaMKII in resting sensory neurons. This is consistent with our previous histological observations showing pCaMKII in DRG sensory neurons using a phospho-specific Thr286/287 antibody (Kojundzic et al., 2010). To additionally confirm autonomous CaMKII in resting neurons, we tested CaMKII activity in DRG lysates using the specific peptide substrate AC2. Four DRGs were harvested from a

control animal during cold perfusion with a solution lacking Na^+ and Ca^{2+}, in order to minimize neuronal activation and Ca^{2+} influx. By *in vitro* determination of the Ca^{2+}-independent kinase activity as a fraction of total activity, we identified an autonomous ratio (activity without Ca^{2+}/CaM divided by activity during saturating Ca^{2+}/CaM conditions, 3 replicate determinations) of 37±9%. This confirms ongoing kinase activity in sensory neurons despite resting conditions.

DISCUSSION

A critical role for CaMKII in amplifying I_{Ca} in response to repetitive or sustained depolarization of excitable cells is well documented (Hudmon et al., 2005; Lee et al., 2006; Tang et al., 2012; Xiao et al., 1994; Yuan and Bers, 1994). However, in the absence of preceding pulses of elevated $[Ca^{2+}]_c$, constitutive regulation of ion channels by CaMKII has been observed in only a few settings, including modulation of resting state sodium channel activity in cardiac myocytes (Yoon et al., 2009), and controlling inactivation kinetics, but not peak current, of P/Q-type channels in hippocampal neurons (Jiang et al., 2008). For L-type currents, this divergence of activity-induced *versus* constitutive CaMKII signaling is apparent in cardiac myocytes, which show a prominent effect of CaMKII inhibition on activity-induced I_{Ca} facilitation, whereas I_{Ca} induced immediately after a period of rest is minimally affected (Yuan and Bers, 1994). Similarly, eliminating CaMKII interactions by mutation of specific $Ca_V1.2$ (L-type) channel target residues in the pore-forming α_{1C} subunit (Blaich et al., 2010) or the auxiliary β_{2a} subunit (Grueter et al., 2006) selectively suppresses facilitation of I_{Ca} following prior Ca^{2+} influx, but does not influence the amplitude of I_{Ca} upon initial depolarization of the resting membrane. Our findings contrast with these reports in showing that unlike L- and P/Q-type channels, ongoing CaMKII activity amplifies the function of N-type channels in resting sensory neurons, a finding that was observed using both a small molecule and a myristoylated peptide inhibitor of CaMKII *in vitro*, and confirmed using AAV transduction of the peptide inhibitor *in vivo*.

Our initial exploration of mechanisms by which CaMKII regulates I_{Ca} of mixed VGCCs in resting neurons shows only a small leftward shift to lower activation voltages, as has been previously shown for the action of CaMKII on L-type channels (Yuan and Bers, 1994). However, this shift is minor in extent and was not observed in isolated N-type currents, which make it likely that the main mechanism by which CaMKII increases I_{Ca} is elevation of channel open probability, comparable to that shown in L-type channels (Dzhura et al., 2000; Grueter et al., 2006). Unlike for P/Q current in hippocampal neurons (Jiang et al., 2008), we did not observe accelerated current inactivation during sustained depolarization following CaMKII inhibition. We also determined that CaMKII inhibition, both acutely *in vitro* and in a sustained fashion *in vivo*, selectively disrupts only N-type channel activity. Although CaMKII enhances I_{Ca} through L-type channels during depolarization of other cell types as noted above, we found no evidence that CaMKII supports L-type I_{Ca} in resting sensory neurons. While we did not selectively examine P/Q-current modulation in the present study, we have previously shown that this current subtype comprises only approximately 15% of total voltage-gated I_{Ca} in sensory neurons (McCallum et al., 2011), suggesting that these channels can not account for the percent I_{Ca} loss we have observed with CaMKII inhibition. This conclusion is supported by the fact that elimination of N-type

current precludes any effect of CaMKII inhibition upon I_{Ca} (Fig. 3C). Together, these data support our conclusion that the N-type channel is the major VGCC effector of CaMKII signaling in sensory neurons at rest, which is concordant with our previous finding in sensory neurons of selective participation of N-type current in CaMKII-mediated facilitation of I_{Ca} in the period immediately following intense neuronal activation and Ca^{2+} influx (Tang et al., 2012).

Our results indicate that CaMKII functions to modulate N-type VGCC activity in sensory neurons despite long intervals of neuronal quiescence. Specifically, to duplicate natural conditions of resting sensory neurons, the dissociated neurons in our preparation rested for at least 2 hours after plating prior to recording. To determine responses, single test depolarizations were used at one-minute intervals, and Ca^{2+} influx was prevented by the use of Ba^{2+} as the charge carrier in the bath. Although our previous findings show that augmented CaMKII signaling resolves within minutes after even sustained depolarization in a Ca^{2+}-containing external solution (Tang et al., 2012), the neurons in our preparation nonetheless displayed ongoing constitutive CaMKII activity. Our finding of comparable CaMKII activity even in neurons from DRGs harvested after first perfusing the intact animal with cold Na^{+}-free, reduced-Ca^{2+} solution makes it unlikely that this basal CaMKII signaling is a result of neuronal activation during tissue harvest, although it could represent residual activated CaMKII persisting from prior sensory stimulation *in vivo*. We therefore postulate that even with long bouts of functional dormancy that characterize healthy peripheral sensory neurons, a basal level of CaMKII activity persists naturally in resting neurons and is essential for maintenance of N-type channel function. How this CaMKII activity is maintained over a long time frame without periodic $[Ca^{2+}]_c$ spikes is unknown, but one simple mechanism is a balance of the opposing actions of CaMKII autophosphorylation and phosphatase activity that permits the persistence of activated (auto-phosphorylated) CaMKII during intervals of baseline $[Ca^{2+}]_c$. Since KN-93 blocks only Ca^{2+}-calmodulin-dependent CaMKII activation and is unable to block Ca^{2+}-independent CaMKII activity, it is unexpected that KN-93 would inhibit CaMKII function in low $[Ca^{2+}]_c$ if CaMKII reactivation was strictly yoked to a traditional Ca^{2+}-CaM activation cycle. Although we attempted to address potential off-target KN-93 activity by always pairing these studies with the inactive analog KN-92, one explanation for our findings is that KN-93 is inhibiting another target in low calcium. However, the fact that we see similar findings with the peptide CaMKII inhibitor AIP supports the notion of an ongoing cycle of CaMKII phosphorylation and dephosphorylation even in low $[Ca^{2+}]_c$. Whether a population of CaMKII is targeted to a nanodomain where $[Ca^{2+}]_c$ is adequate for calmodulin-reactivation of CaMKII despite chelators, or whether CaMKII can be reactivated by calmodulin in sensory neurons independent of a traditional Ca^{2+}-calmodulin cycle, require further investigation.

The use-dependent component of CaMKII activity provides negative feedback control of neuronal excitability by increasing I_{Ca} (Lirk et al., 2008; Tang et al., 2012). In contrast, the utility of sustained CaMKII activity in a resting neuron may be to maintain the calcium signaling machinery in a ready state. In addition, a basal level of CaMKII activity may be important as a homeostatic mechanism related to neuronal survival. A minimal level of

CaMKII activity has been shown to be necessary to prevent the demise of various central and peripheral neuron populations (Ashpole and Hudmon, 2011; Ashpole et al., 2012; Bok et al., 2007), in which a critical level of CaMKII function is maintained by periodic neuronal firing and Ca^{2+} entry through VGCCs (Bok et al., 2007; Catsicas et al., 1992; Furber et al., 1987; Hegarty et al., 1997; Lipton, 1986; Ruijter et al., 1991). However, sensory neurons *in situ* are naturally inactive in the absence of specific sensory stimulation (Bessou and Perl, 1969). Without ongoing electrical activity, a moderate level of basal CaMKII function may be a means by which sensory neurons maintain pro-survival effects without requiring regular membrane depolarizations that would confound their basic sensory function.

CaMKII is ideally designed to detect excitation events in neurons equipped with N-type VGCCs, and to encode this into enhanced I_{Ca} (Tang et al., 2012). Our present findings indicate that this response mode is superimposed on a base of ongoing CaMKII activity that is independent of depolarization-related Ca^{2+} elevation. Since the extent of I_{Ca} loss when CaMKII is inhibited in resting neurons is comparable to the increase of I_{Ca} when CaMKII is activated by intense sensory neuron firing (Tang et al., 2012), it appears that the CaMKII/N-type Ca^{2+} channel regulatory system has been optimized to function in the middle of its dynamic range in resting neurons, suggesting a critical regulatory role for this system.

Acknowledgments

The study was supported by National Institutes of Health Grant NS-42150 (to Q.H.H.)

ABBREVIATIONS

AAV	Adeno-associated virus
AIP	Autocamtide-2-related inhibitory peptide
CaMKII	Calcium/calmodulin-dependent protein kinase II
DMSO	Dimethyl sulfoxide
DRG	Dorsal root ganglion
EGFP	Enhanced GFP
EGTA	Ethylene glycol tetraacetic acid
HEPES	2-[4-(2-hydroxyethyl)piperazin-1-yl]ethanesulfonic acid
HVA	High-voltage-activated
LVA	Low voltage activated
mCl	Myristoyl-chloride
mAIP	Myristoylated autocamtide-2-related inhibitory peptide
MVIIC	ω-conotoxin MVIIC
VGCCs	Voltage-gated Ca^{2+} channels

References

Ashpole NM, Hudmon A. Excitotoxic neuroprotection and vulnerability with CaMKII inhibition. Mol Cell Neurosci. 2011; 46:720–730. [PubMed: 21316454]

Ashpole NM, Song W, Brustovetsky T, Engleman EA, Brustovetsky N, Cummins TR, Hudmon A. Calcium/calmodulin-dependent protein kinase II (CaMKII) inhibition induces neurotoxicity via dysregulation of glutamate/calcium signaling and hyperexcitability. J Biol Chem. 2012; 287:8495–8506. [PubMed: 22253441]

Berridge MJ. Neuronal calcium signaling. Neuron. 1998; 21:13–26. [PubMed: 9697848]

Bessou P, Perl ER. Response of cutaneous sensory units with unmyelinated fibers to noxious stimuli. Journal of neurophysiology. 1969; 32:1025–1043. [PubMed: 5347705]

Blaich A, Welling A, Fischer S, Wegener JW, Kostner K, Hofmann F, Moosmang S. Facilitation of murine cardiac L-type Ca(v)1.2 channel is modulated by calmodulin kinase II-dependent phosphorylation of S1512 and S1570. Proc Natl Acad Sci U S A. 2010; 107:10285–10289. [PubMed: 20479240]

Bok J, Wang Q, Huang J, Green SH. CaMKII and CaMKIV mediate distinct prosurvival signaling pathways in response to depolarization in neurons. Mol Cell Neurosci. 2007; 36:13–26. [PubMed: 17651987]

Catsicas M, Pequignot Y, Clarke PG. Rapid onset of neuronal death induced by blockade of either axoplasmic transport or action potentials in afferent fibers during brain development. J Neurosci. 1992; 12:4642–4650. [PubMed: 1281491]

Dzhura I, Wu Y, Colbran RJ, Balser JR, Anderson ME. Calmodulin kinase determines calcium-dependent facilitation of L-type calcium channels. Nat Cell Biol. 2000; 2:173–177. [PubMed: 10707089]

Fischer G, Kostic S, Nakai H, Park F, Sapunar D, Yu H, Hogan Q. Direct injection into the dorsal root ganglion: technical, behavioral, and histological observations. J Neurosci Methods. 2011; 199:43–55. [PubMed: 21540055]

Fossat P, Dobremez E, Bouali-Benazzouz R, Favereaux A, Bertrand SS, Kilk K, Leger C, Cazalets JR, Langel U, Landry M, Nagy F. Knockdown of L calcium channel subtypes: differential effects in neuropathic pain. J Neurosci. 2010; 30:1073–1085. [PubMed: 20089916]

Fuchs A, Lirk P, Stucky C, Abram SE, Hogan QH. Painful nerve injury decreases resting cytosolic calcium concentrations in sensory neurons of rats. Anesthesiology. 2005; 102:1217–1225. [PubMed: 15915036]

Furber S, Oppenheim RW, Prevette D. Naturally-occurring neuron death in the ciliary ganglion of the chick embryo following removal of preganglionic input: evidence for the role of afferents in ganglion cell survival. J Neurosci. 1987; 7:1816–1832. [PubMed: 3598650]

Grimm D, Zhou S, Nakai H, Thomas CE, Storm TA, Fuess S, Matsushita T, Allen J, Surosky R, Lochrie M, Meuse L, McClelland A, Colosi P, Kay MA. Preclinical in vivo evaluation of pseudotyped adeno-associated virus vectors for liver gene therapy. Blood. 2003; 102:2412–2419. [PubMed: 12791653]

Grueter CE, Abiria SA, Dzhura I, Wu Y, Ham AJ, Mohler PJ, Anderson ME, Colbran RJ. L-type Ca2+ channel facilitation mediated by phosphorylation of the beta subunit by CaMKII. Mol Cell. 2006; 23:641–650. [PubMed: 16949361]

Hardcastle J, Hardcastle PT, Noble JM. The secretory action of barium chloride in rat colon. J Physiol. 1985; 361:19–33. [PubMed: 3989726]

Hegarty JL, Kay AR, Green SH. Trophic support of cultured spiral ganglion neurons by depolarization exceeds and is additive with that by neurotrophins or cAMP and requires elevation of [Ca2+]i within a set range. J Neurosci. 1997; 17:1959–1970. [PubMed: 9045725]

Heinke B, Balzer E, Sandkuhler J. Pre- and postsynaptic contributions of voltage-dependent Ca2+ channels to nociceptive transmission in rat spinal lamina I neurons. Eur J Neurosci. 2004; 19:103–111. [PubMed: 14750968]

Hell JW, Appleyard SM, Yokoyama CT, Warner C, Catterall WA. Differential phosphorylation of two size forms of the N-type calcium channel alpha 1 subunit which have different COOH termini. J Biol Chem. 1994; 269:7390–7396. [PubMed: 8125957]

Hell JW, Yokoyama CT, Wong ST, Warner C, Snutch TP, Catterall WA. Differential phosphorylation of two size forms of the neuronal class C L-type calcium channel alpha 1 subunit. J Biol Chem. 1993; 268:19451–19457. [PubMed: 8396138]

Hudmon A, Schulman H, Kim J, Maltez JM, Tsien RW, Pitt GS. CaMKII tethers to L-type Ca2+ channels, establishing a local and dedicated integrator of Ca2+ signals for facilitation. The Journal of cell biology. 2005; 171:537–547. [PubMed: 16275756]

Ishida A, Fujisawa H. Stabilization of calmodulin-dependent protein kinase II through the autoinhibitory domain. J Biol Chem. 1995; 270:2163–2170. [PubMed: 7836445]

Ishida A, Kameshita I, Okuno S, Kitani T, Fujisawa H. A novel highly specific and potent inhibitor of calmodulin-dependent protein kinase II. Biochem Biophys Res Commun. 1995; 212:806–812. [PubMed: 7626114]

Jagodic MM, Pathirathna S, Joksovic PM, Lee W, Nelson MT, Naik AK, Su P, Jevtovic-Todorovic V, Todorovic SM. Upregulation of the T-type calcium current in small rat sensory neurons after chronic constrictive injury of the sciatic nerve. Journal of neurophysiology. 2008; 99:3151–3156. [PubMed: 18417624]

Jiang X, Lautermilch NJ, Watari H, Westenbroek RE, Scheuer T, Catterall WA. Modulation of CaV2.1 channels by Ca2+/calmodulin-dependent protein kinase II bound to the C-terminal domain. Proc Natl Acad Sci U S A. 2008; 105:341–346. [PubMed: 18162541]

Kojundzic SL, Puljak L, Hogan Q, Sapunar D. Depression of Ca(2+)/calmodulin-dependent protein kinase II in dorsal root ganglion neurons after spinal nerve ligation. J Comp Neurol. 2010; 518:64–74. [PubMed: 19882720]

Kolb SJ, Hudmon A, Waxham MN. Ca2+/calmodulin kinase II translocates in a hippocampal slice model of ischemia. J Neurochem. 1995; 64:2147–2156. [PubMed: 7722499]

Lee TS, Karl R, Moosmang S, Lenhardt P, Klugbauer N, Hofmann F, Kleppisch T, Welling A. Calmodulin kinase II is involved in voltage-dependent facilitation of the L-type Cav1.2 calcium channel: Identification of the phosphorylation sites. J Biol Chem. 2006; 281:25560–25567. [PubMed: 16820363]

Lipton SA. Blockade of electrical activity promotes the death of mammalian retinal ganglion cells in culture. Proc Natl Acad Sci U S A. 1986; 83:9774–9778. [PubMed: 3025849]

Lirk P, Poroli M, Rigaud M, Fuchs A, Fillip P, Huang CY, Ljubkovic M, Sapunar D, Hogan Q. Modulators of calcium influx regulate membrane excitability in rat dorsal root ganglion neurons. Anesth Analg. 2008; 107:673–685. [PubMed: 18633052]

McCallum JB, Kwok WM, Mynlieff M, Bosnjak ZJ, Hogan QH. Loss of T-type calcium current in sensory neurons of rats with neuropathic pain. Anesthesiology. 2003; 98:209–216. [PubMed: 12502999]

McCallum JB, Wu HE, Tang Q, Kwok WM, Hogan QH. Subtype-specific reduction of voltage-gated calcium current in medium-sized dorsal root ganglion neurons after painful peripheral nerve injury. Neuroscience. 2011; 179:244–255. [PubMed: 21277351]

Mironov SL, Usachev Y. Sr and Ba transients in isolated snail neurones studied with fura-2. The recovery from depolarization induced load and modulation of Ca release from intracellular stores. Neurosci Lett. 1990; 112:184–189. [PubMed: 2132298]

Nelson MT, Joksovic PM, Perez-Reyes E, Todorovic SM. The endogenous redox agent L-cysteine induces T-type Ca2+ channel-dependent sensitization of a novel subpopulation of rat peripheral nociceptors. J Neurosci. 2005; 25:8766–8775. [PubMed: 16177046]

Park J, Luo ZD. Calcium channel functions in pain processing. Channels (Austin). 2010; 4:510–517. [PubMed: 21150297]

Ruijter JM, Baker RE, De Jong BM, Romijn HJ. Chronic blockade of bioelectric activity in neonatal rat cortex grown in vitro: morphological effects. Int J Dev Neurosci. 1991; 9:331–338. [PubMed: 1950648]

Sapunar D, Ljubkovic M, Lirk P, McCallum JB, Hogan QH. Distinct membrane effects of spinal nerve ligation on injured and adjacent dorsal root ganglion neurons in rats. Anesthesiology. 2005; 103:360–376. [PubMed: 16052119]

Takahashi T, Momiyama A. Different types of calcium channels mediate central synaptic transmission. Nature. 1993; 366:156–158. [PubMed: 7901765]

Tang Q, Bangaru ML, Kostic S, Pan B, Wu HE, Koopmeiners AS, Yu H, Fischer GJ, McCallum JB, Kwok WM, Hudmon A, Hogan QH. Ca(2)(+)-dependent regulation of Ca(2)(+) currents in rat primary afferent neurons: role of CaMKII and the effect of injury. J Neurosci. 2012; 32:11737–11749. [PubMed: 22915116]

TerBush DR, Holz RW. Barium and calcium stimulate secretion from digitonin-permeabilized bovine adrenal chromaffin cells by similar pathways. J Neurochem. 1992; 58:680–687. [PubMed: 1729410]

Todorovic SM, Lingle CJ. Pharmacological properties of T-type Ca2+ current in adult rat sensory neurons: effects of anticonvulsant and anesthetic agents. Journal of neurophysiology. 1998; 79:240–252. [PubMed: 9425195]

Welsby PJ, Wang H, Wolfe JT, Colbran RJ, Johnson ML, Barrett PQ. A mechanism for the direct regulation of T-type calcium channels by Ca2+/calmodulin-dependent kinase II. J Neurosci. 2003; 23:10116–10121. [PubMed: 14602827]

Wolfe JT, Wang H, Perez-Reyes E, Barrett PQ. Stimulation of recombinant Ca(v)3.2, T-type, Ca(2+) channel currents by CaMKIIgamma(C). J Physiol. 2002; 538:343–355. [PubMed: 11790804]

Xiao RP, Cheng H, Lederer WJ, Suzuki T, Lakatta EG. Dual regulation of Ca2+/calmodulin-dependent kinase II activity by membrane voltage and by calcium influx. Proc Natl Acad Sci U S A. 1994; 91:9659–9663. [PubMed: 7937825]

Yoon JY, Ho WK, Kim ST, Cho H. Constitutive CaMKII activity regulates Na+ channel in rat ventricular myocytes. J Mol Cell Cardiol. 2009; 47:475–484. [PubMed: 19591836]

Yuan W, Bers DM. Ca-dependent facilitation of cardiac Ca current is due to Ca- calmodulin-dependent protein kinase. Am J Physiol. 1994; 267:H982–993. [PubMed: 8092302]

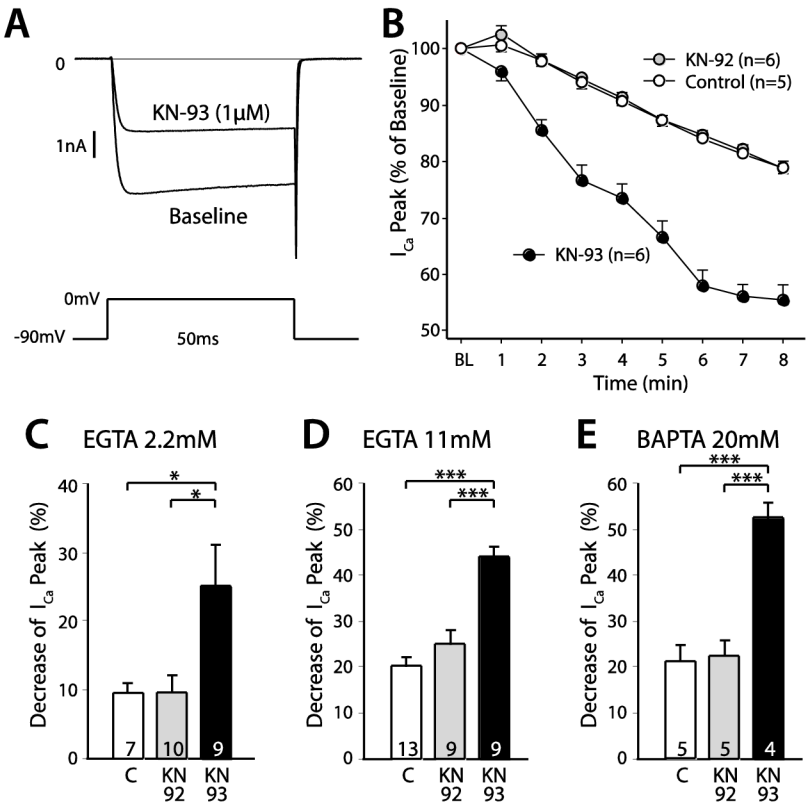

Figure 1.

Effect of CaMKII inhibitor KN-93 on voltage-gated I_{Ca}. **(A)** Sample I_{Ca} traces (top) in response to step depolarizations (bottom) demonstrate decreased peak current during application of KN-93 (4.57nA) compared to baseline in the same neuron (6.03nA). **(B)** Time course of onset of blockade by KN-93 in comparison to KN-92 and controls exposed to vehicle (0.1% DMSO) alone. **(C)** Using a standard internal pipette solution with 2.2mM EGTA, KN-93 ("KN93", 1μM) applied for 5 minutes decreased I_{Ca} peak (as a percentage of baseline), compared to change in time-matched control neurons ("C") and the application of the inactive isomer KN-92 ("KN92"). Baseline I_{Ca} peak was 125.8±4.9pA/pF and did not differ between treatment groups. **(D)** With pipette solution containing11mM EGTA, KN-93 (1μM) suppressed peak I_{Ca}, while KN-92 did not. Baseline I_{Ca} peak was 104.6±6.0pA/pF and did not differ between treatment groups. **(E)** Further buffering by the addition of 20mM BAPTA showed similar results. Baseline I_{Ca} peak was 144.9±17.1pA/pF and did not differ between treatment groups. Data for groups are mean ± SEM; numbers in bars are n for each group; * P<0.05, *** P<0.001 for Tukey's test.

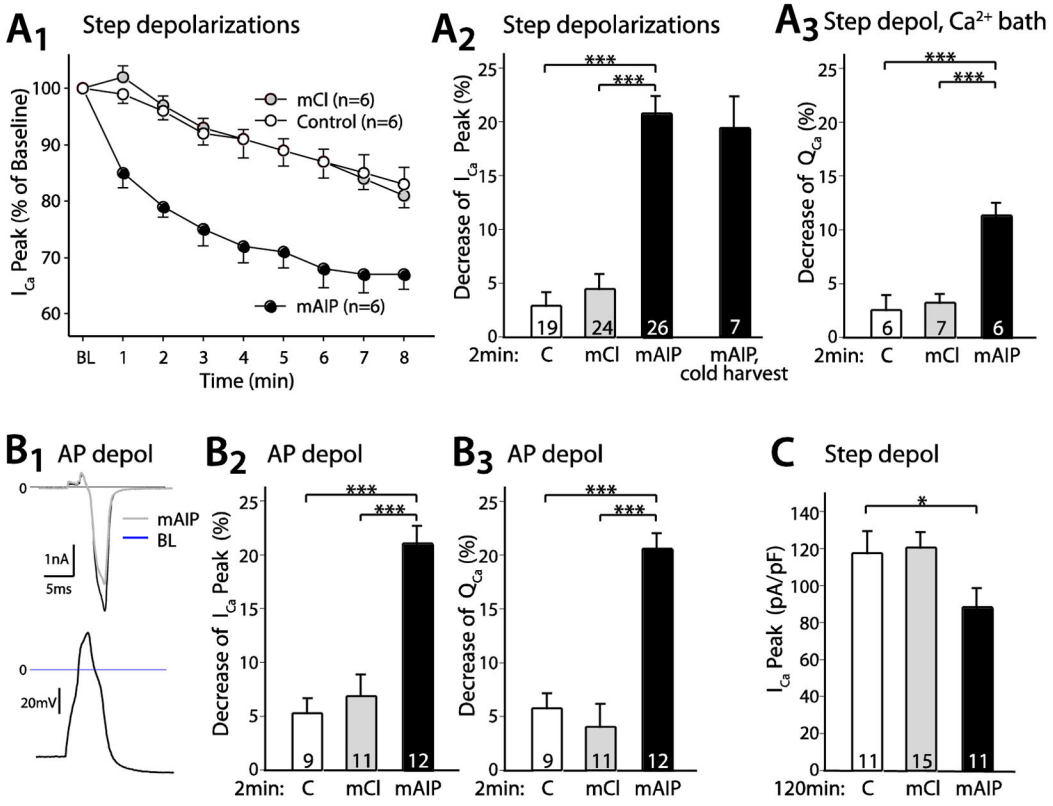

Figure 2.

Effect of CaMKII inhibitor myristoylated autocamtide-2-related inhibitory peptide ("mAIP") on voltage-gated I_{Ca}. **(A_1)** Peak I_{Ca} induced by step depolarization from −60mV to 0mV was determined at baseline and each minute thereafter for neurons exposed to mAIP (5μM), myristoyl chloride ("mCl", 5μM), or control neurons without any agent. The decrease in normalized I_{Ca} for mAIP maximally diverged from both other groups by 2 minutes. **(A_2)** Summary data show that application (2min) of mAIP depressed peak I_{Ca} evoked by step depolarizations, whereas mCl had no effect compared to time controls ("C"). Collection of tissue in a fashion that minimized neuronal Ca^{2+} influx by using ice-cold perfusate that lacked Na^+ and had minimal Ca^{2+} ("cold harvest") did not alter the efficacy of mAIP compared to the conventional tissue harvest. Baseline I_{Ca} peak was 104.7±3.7pA/pF and did not differ between groups. **(A_3)** In a bath solution containing Ca^{2+} (2mM) rather than Ba^{2+}, mAIP again selectively blocked I_{Ca}. Baseline I_{Ca} peak was 86.4±4.8pA/pF and did not differ between groups. **(B_1)** Sample I_{Ca} traces (top) in response to action potential (AP) waveform depolarizations (bottom) demonstrate depression of the peak current in the mAIP trace (3.17nA) compared to the baseline ("BL") trace (4.05nA). Total charge transfer (Q_{Ca}) was also depressed by mAIP (7.34nA•ms) compared to BL (9.07nA•ms). The group of neurons treated with mAIP showed a loss of both I_{Ca} peak **(B_2)** and Q_{Ca} **(B_3)**, whereas there were no changes in the Control ("C") or mCl groups. Baseline I_{Ca} peak was 109.4±8.3pA/pF, while baseline Q_{Ca} was 249±18pA/pF•ms, neither of which differed between treatment groups. **(C)** Neurons incubated for 120min in mAIP had reduced peak I_{Ca} induced by step depolarizations compared to Controls, whereas mCl has no effect. (Note:

unlike the adjacent graphs, current density rather than % change is reported in this graph because pre-incubation values were not available to determine the effect of the agents on a normalized basis.) Data for groups are mean ± SEM; numbers in bars are n for each group; * $P<0.05$, *** $P<0.001$ for Tukey's test.

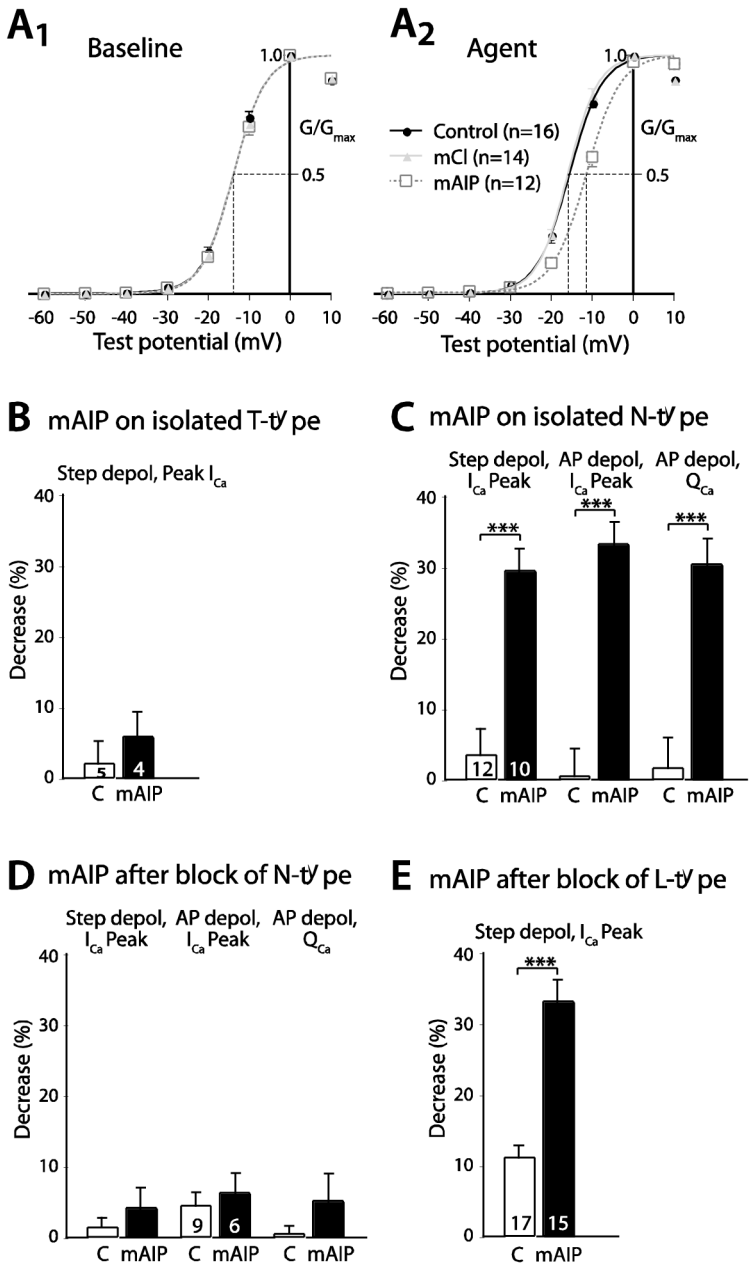

Figure 3.

CaMKII differentially regulates voltage-gated Ca^{2+} channel function and subtypes. **(A)** Activation curves for averaged data (mean ± SEM) of each group fitted to the Boltzmann function for neurons at baseline **(A_1)** and following application of myristoylated autocamtide-2-related inhibitory peptide (“mAIP”, 5μM), myristoyl chloride (“mCl”, 5μM), or time-matched Control **(A_2)**. The $V_{1/2}$ in the mAIP group was significantly (P<0.001) shifted in a depolarizing direction (-11.4±0.3mV) compared to the mCl (15.9±0.2mV) and time Control groups (15.5±0.3mV). **(B)** T-type current was measured by isolation with HVA current blockers (20min incubation with SNX-482, 200nM, and MVIIC, 200nM, and recording in a bath containing nimodipine, 5uM, and ω-Conotoxin GVIA, 200nM), and

evoking I_{Ca} by step depolarizations from a holding potential of −100mV to a test potential of −30mV. The current peak was corrected by subtracting the sustained component (Jagodic et al., 2008). Application of mAIP has minimal effect on peak T-type I_{Ca} that is not different from the time control. **(C)** During isolation of N-type current by application of selective blockers of other VGCC subtypes (nisoldipine 200nM for L-type, SNX-482 500nM for components of R-type, and temporary application of ω-conotoxin MVIIC 2μM for persisting block of P/Q-type), I_{Ca} was measured before and after exposure to mAIP, and compared to time-matched Control neurons that were exposed only to continued application of the VGCC blockers without added mAIP. Percent blockade was determined as the I_{Ca} blocked by mAIP (or lost during a comparable time interval) divided by the difference between baseline I_{Ca} and that which remained after application of SNX-111 (200nM) at the end of each experiment, multiplied by 100. Myristoylated AIP (mAIP) decreased peak I_{Ca} elicited by step depolarization, peak I_{Ca} during AP-waveform depolarization, and total charge transfer (Q_{Ca}) during AP-waveform depolarization. Baseline measures of step-induced peak I_{Ca} (57.7±4.1pA/pF), AP-waveform-induced peak I_{Ca} (109.4±8.3pA/pF) and waveform-induced Q_{Ca} (249.4±17.8pA/pF•ms) did not differ between groups. **(D)** Prior treatment of neurons with SNX-111 alone eliminated the effect of mAIP application on all three measures of I_{Ca}. Baseline measures of step-induced peak I_{Ca} (101.9±7.5pA/pF), AP-waveform-induced peak I_{Ca} (183.6±12.2pA/pF) and waveform-induced Q_{Ca} (440.1±29.0pA/pF•ms) did not differ between groups. Block of I_{Ca} by SNX-111 for these three measures (63.4±1.8%, 67.9±1.6%, and 67.5±1.6%) did not differ between groups. **(E)** Application of nisoldipine (200nM) in the recording bath did not preclude suppression of step-evoked I_{Ca} peak by subsequently applied mAIP. Baseline peak I_{Ca} (82.9±7.1pA/pF) and the percentage of current blocked by nisoldipine (22.4±2.2%) did not differ between groups. Mean ± SEM; *** P<0.001 for t-tests.

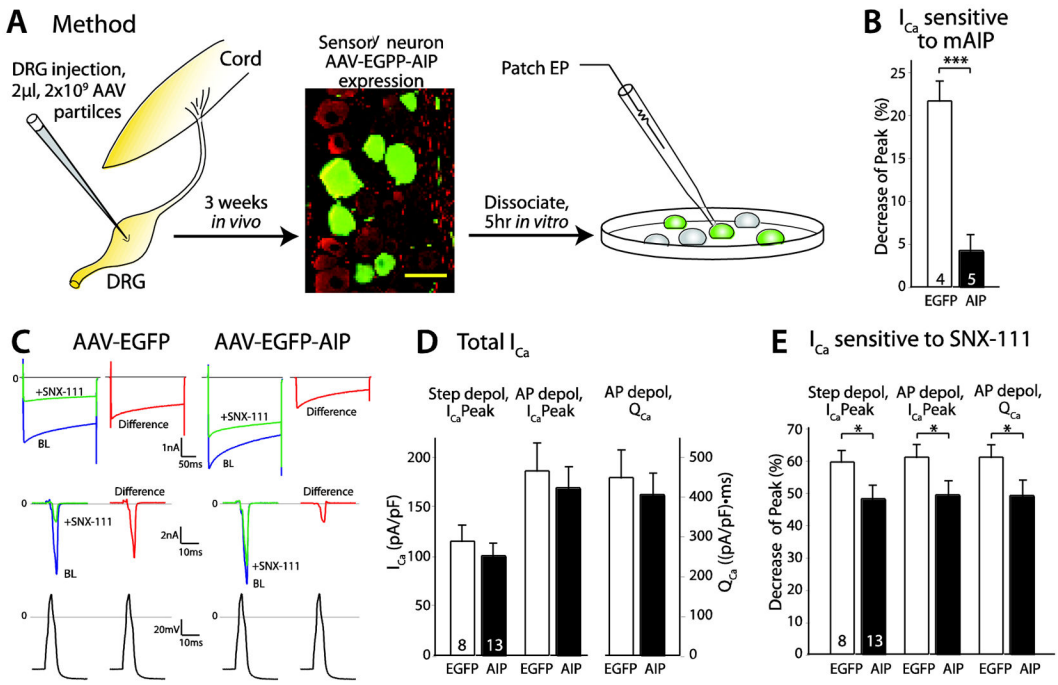

Figure 4.

In vivo blockade of CaMKII by expression of AIP. **(A)** The method involves injection of adeno-associated virus (AAV) vector into the dorsal root ganglion (DRG) of the anesthetized rat, *in vivo* transduction and transgene expression for 3 weeks (green, EGFP; red, β3-Tubulin), followed by DRG harvest and neuronal dissociation for electrophysiological study. Scale bar 50µm. **(B)** Neurons expressing EGFP alone ("EGFP") retain sensitivity of I_{Ca} to CaMKII blockade with mAIP (5µM) that is comparable to Control neurons (Fig. $2A_2$), whereas neurons expressing EGFP-AIP ("AIP") have reduced sensitivity to CaMKII blockade. **(C)** Sample traces of currents elicited by step depolarizations (top row) and by action potential ("AP") waveform commands (currents in middle row, voltage commands in the bottom row) show I_{Ca} at baseline ("BL"), I_{Ca} in the same neuron after N-type I_{Ca} block with SNX-111 (200nM), and the difference current sensitive to SNX-111 obtained by subtraction. Recordings are shown from a neuron expressing only EGFP (left) and another expressing EGFP-AIP (right). **(D)** Neurons expressing either EGFP alone ("EGFP") or EGFP-AIP ("AIP") did not differ in peak I_{Ca} measured by step depolarization (left bars) or AP waveform depolarization (middle bars), and charge transfer (Q_{Ca}) was also unaffected (right bars, ordinate scale to the right). **(E)** Block of I_{Ca} by SNX-111 application was compared in neurons expressing EGFP alone or EGFP-AIP. Less I_{Ca} blockade (i.e. less N-type I_{Ca}) was evident in neurons expressing EGFP-AIP by all three measures. Mean ± SEM; * $P<0.05$ for t-tests.